



Article

Liquid Crystalline Mixtures with Induced Polymorphic Smectic Phases Targeted for Energy Investigations

Salma A. Al-Zahrani ¹, Mohd Taukeer Khan ² , Violeta Jevtovic ¹ , Najat Masood ¹, Yassin Aweis Jeilani ¹, Hoda A. Ahmed ^{3,4,*}  and Fatimah M. Alfaidi ⁴

¹ Chemistry Department, Faculty of Science, University of Ha'il, P.O. Box 2440, Ha'il 81451, Saudi Arabia; s.alzahrane@uoh.edu.sa (S.A.A.-Z.); v.jevtovic@uoh.edu.sa (V.J.); ne.ebrahim@uoh.edu.sa (N.M.); ya.jeilani@uoh.edu.sa (Y.A.J.)

² Department of Physics, Faculty of Science, Islamic University of Madinah, Al-Madinah Al-Munawwarah 42351, Saudi Arabia; khanmtk@iu.edu.sa

³ Department of Chemistry, Faculty of Science, Cairo University, Cairo 12613, Egypt

⁴ Chemistry Department, Faculty of Science, Taibah University, Yanbu 46423, Saudi Arabia; fatimahm.alfaidi@gmail.com

* Correspondence: ahoda@sci.cu.edu.eg

Abstract: In this study, 4-Biphenyle-4'-alkyloxybenzenamines were synthesized as a homologous series of liquid crystals based on the biphenyl moiety. Their mesomorphic and optical properties were examined for both pure and mixed components. Elemental analysis, NMR, and FT-IR spectroscopy were used to determine the molecular structures of the developed materials. Using differential scanning calorimetry (DSC), the mesophase transitions were studied, and polarized optical microscopy was used to identify the textures of the mesophases (POM). The obtained results showed that all compounds are dimorphic and only have smectic B (SmB) and smectic A (SmA) phases for all terminal side chains, which are enantiotropic. With variably proportionated terminal side chains and a focus on the mesomorphic temperature range, binary phase diagrams were constructed and an induced smectic C phase was achieved (SmC). It was found that terminal chain length affects both conformation and steric impact in the mixed states. The absorption and fluorescence emission spectra of pure as well as their binary mixtures liquid crystalline films were recorded to investigate the optical and photophysical properties. It was noted that, with the increase in alkyl chain length, the energy bandgap increases from 3.24 eV (for C₆H₁₃) to 3.37 eV (for C₁₆H₃₃) and charge carrier lifetime decreases, ascribing to the increase in steric hindrance causing, consequently, the faster decay of charge carriers.

Keywords: liquid crystals; induced phase; polymorphic; optical properties; thin film; binary phase diagrams; energy bandgap



Citation: Al-Zahrani, S.A.; Khan, M.T.; Jevtovic, V.; Masood, N.; Jeilani, Y.A.; Ahmed, H.A.; Alfaidi, F.M. Liquid Crystalline Mixtures with Induced Polymorphic Smectic Phases Targeted for Energy Investigations. *Crystals* **2023**, *13*, 645. <https://doi.org/10.3390/cryst13040645>

Academic Editor: Waldemar Maniukiewicz

Received: 17 March 2023

Revised: 2 April 2023

Accepted: 7 April 2023

Published: 9 April 2023



Copyright: © 2023 by the authors. Licensee MDPI, Basel, Switzerland. This article is an open access article distributed under the terms and conditions of the Creative Commons Attribution (CC BY) license (<https://creativecommons.org/licenses/by/4.0/>).

1. Introduction

Due to their fascinating optical properties, which enable numerous electro-optical applications such as optical storage devices, switching, and holography, liquid crystalline materials with a Schiff base moiety in the mesogenic part of monomers, dimers, oligomers, or polymeric in nature are frequently studied [1–10]. The phase behavior and optical features of numerous LC materials are controlled for such materials using the photochromic azomethine group phenomena [11–15]. The reversible trans–cis isomerization caused by ultraviolet radiation stabilizes the LC's mesophase structure by bringing about molecular ordering in the trans isomer, whereas disordering the cis isomer disrupts the phase structure. As a result, the cis isomer will have a lower clearing point than the trans one [15–17].

According to reports, the central linkages, terminal groups, and molecular structures all play significant roles in the formation, character, thermal stability, and temperature range of the liquid crystalline compound's mesophase [18–33]. J. Goodby et al. have

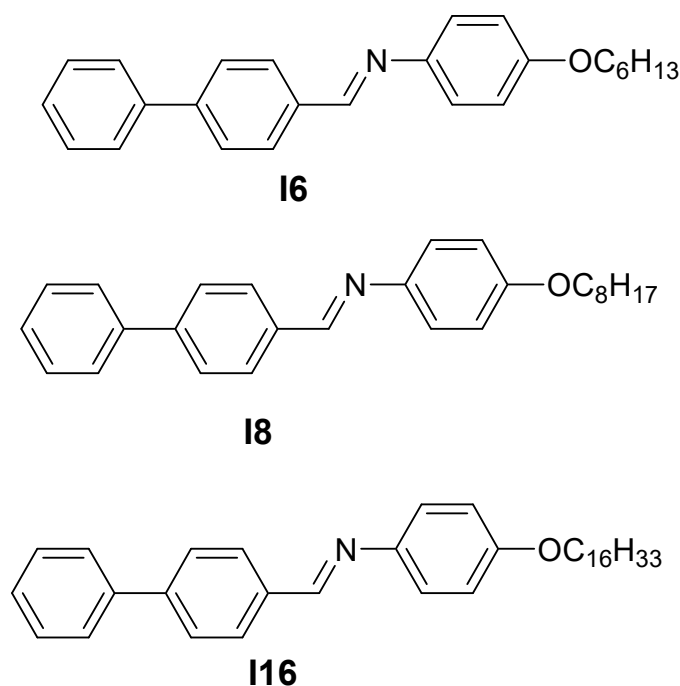
illustrated the impact of the reduction of the free volume on the mesophases of the LCs, for example, (a) SmA phases with variable layer spacing, (b) SmC phases without layer shrinkage, and (c) lattice structures of available space and fibers in twist-bend nematic phase [34].

Calamitic molecules are linear and have two terminal groups, which may or may not be the same. In the construction of LCs, a variety of wings units have been created, but the most common method [35] is to utilize an alkyl/alkoxy chain or a short, compact polar substituent [36–39]. These groups serve as a dipolar component that introduces anisotropy in physical properties. Several interesting investigations [40–47] have produced liquid crystal-based Schiff base linkages and examined them. A mesogenic core, connecting group, and terminal functional substituent must be carefully chosen in order to build and investigate novel advanced functional thermotropic liquid crystal materials [48].

From the viewpoint of its applications, liquid crystals (LCs) have attracted significant interest. They are recognized for their unique textures as well [49]. A certain set of properties, such as viscosity, birefringence, dielectric anisotropy, and elastic constants within a certain range, are necessary for a particular application of a liquid crystalline substance. A single LC might not be able to satisfy every requirement of a specific application. In order to maximize the required physical properties for a given application and to support the thermal stability of their mesophases, liquid crystalline mixes of two or more compounds are typically used [49–51]. Eutectic blends of two or more LC materials are in large-scale use in display technology; these mixtures have the lowest melting temperature. A binary mixture made up of two LC components is the most basic type of mixture. The development of a considerably more ordered induced smectic phase from components that only exhibit nematic phase in their pure forms is an attractive characteristic of binary or multi-component LC mixtures [52–56]. A binary mixture made up of two LC components is the most basic type of mixture. The creation of a considerably more ordered induced smectic phase from components that only exhibit nematic phase in their pure forms is an attractive characteristic of binary or multi-component LC mixtures [52–56].

The linearity of the biphenyl group is maintained despite its stepped shape, making it more stable and enabling the mesophase to develop. Furthermore, non-symmetrical biphenyl derivatives' mesophase behavior has recently been studied [57,58]. A new linking group was also added, and the rigidity component suffered a modification, which stabilized the mesomorphic behavior and may have resulted in the appearance of new phases [59,60].

Materials that exhibit their mesophases at room temperature and maintain their liquid crystalline characteristics over a large temperature range are desirable for practical applications. Utilizing mixtures is one approach to this because, in these cases, the mesophase–isotropic line is linearly or slightly improved with composition [61–66]. Additionally, the low-melting eutectic combination has a wider temperature range for the mesophase at the eutectic composition than either of the two pure components. In order to develop phase diagram mixtures, specific liquid crystal derivatives were designed. This was performed for two reasons: first, they can induce liquid crystalline phases when mixed with them and, second, they can significantly alter the phase behavior of liquid crystalline materials when mixed with mesomorphic materials, as has recently been demonstrated for the induction of liquid crystal phases [62,63]. The purpose of the current research is to design three rings of liquid crystals based on derivatives of the biphenyl moiety (Scheme 1) and to analyze their thermal and optical characteristics in pure and mixed states. The mesophase of their binary mixtures generated from any two extreme homologues with varying alkoxy chain lengths should also be investigated (n). The absorption spectra, steady-state, and time-resolved fluorescence spectra of developed samples were used to evaluate the optical and photophysical properties for pure and blended components.



Scheme 1. Investigated mesomorphic compounds, **In**.

2. Results and Discussion

2.1. Mesomorphic and Binary Phase Mixture Investigations

Transition temperatures for the prepared homologues **In**, as given in previous investigations, Ref. [66], are collected in Supplementary S1. As can be seen from the table, according to the increase in temperature, the related endotherms were recognized as the following: crystalline to SmB, SmB to SmA, and SmA–isotropic phase transitions. All synthesized homologues **I6**, **I8**, and **I16** are dimorphic possessing enantiotropic SmB and SmA mesophases. The presence of the typical textures acted as a defining characteristic of the SmB and SmA mesophases [66].

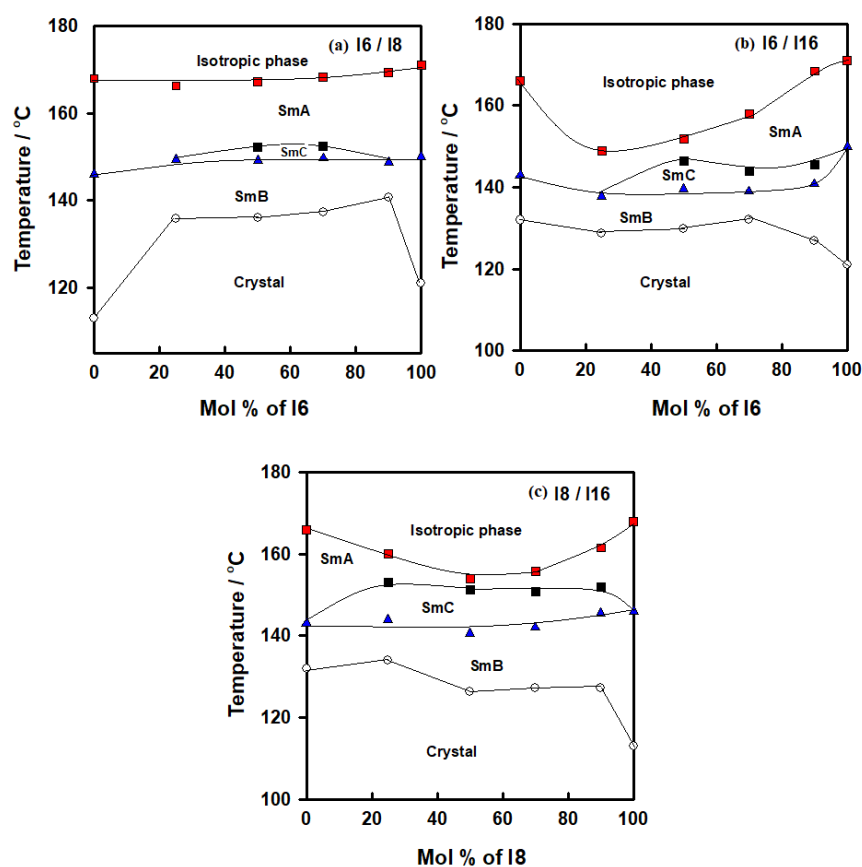
In general, molecular–molecular interactions, along with the stereo and/or mesomeric features of the molecule, have a direct impact on the mesomorphic trend of a certain calamitic mesogen. The molecular association of the rod-like molecules in the current series of compounds and, subsequently, their mesophase thermal stability, whether in their pure or mixed states, are primarily influenced by different interfering variables in, first, increased lateral adhesion of linear molecules as the length of terminal alkoxy chain increases (*n*). Secondly, the end-to-end connection varies depending on the polarity of the terminal substituent, and produces various mesomeric effects, which in turn produce various dipole–dipole interactions and, finally, the molecular structure of the whole molecule. These factors are shared in various ratios to the mesophase behavior of the different binary mixtures investigated.

Table 1 lists the transitional temperatures and their related enthalpies for three homologous binary mixing systems (**I6/I8**, **I6/I16**, and **I8/I16**). Previous reports on specific chemicals exist [66]. Figure 1a–c graphically illustrates the temperature transitions of the pure compounds as well as their mixtures. As shown in Table 1 and Figure 1, when homologues with varied alkoxy chain lengths were mixed, they all displayed enantiotropic characteristics that applied to all compositions.

Table 1. Phase transitional temperatures ($^{\circ}\text{C}$) and related enthalpies ΔH , kJ/g for binary mixtures.

% Compound (System I6/I8)	$T_{\text{Cr-SmB}}$	$\Delta H_{\text{Cr-SmB}}$	$T_{\text{SmB-SmC}}$	$\Delta H_{\text{SmB-SmC}}$	$T_{\text{SmC-SmA}}$	$\Delta H_{\text{SmC-SmA}}$	$T_{\text{SmA-I}}$	$\Delta H_{\text{SmA-I}}$
0% I6	113.0	51.78	146.0	28.11	-	-	168.0	3.22
24% I6	135.9	49.27	149.3	23.22	-	-	166.3	3.27
50% I6	136.0	43.62	149.1	30.25	152.3	4.21	167.2	3.18
75% I6	137.3	50.29	149.7	27.21	152.4	4.36	168.4	3.12
90% I6	140.7	46.20	148.8	21.72	-	-	169.4	3.00
100% I6	121.0	51.00	150.0	25.84	-	-	171.0	3.92
%Compound (System I6/I16)	$T_{\text{Cr-SmB}}$	$\Delta H_{\text{Cr-SmB}}$	$T_{\text{SmB-SmC}}$	$\Delta H_{\text{SmB-SmC}}$	$T_{\text{SmC-SmA}}$	$\Delta H_{\text{SmC-SmA}}$	$T_{\text{SmA-I}}$	$\Delta H_{\text{SmA-I}}$
0% I6	132.0	31.50	143.0	29.91	-	-	166.0	3.00
25% I6	128.7	39.20	137.8	33.92	-	-	148.9	3.95
50% I6	129.9	43.67	139.6	30.20	146.5	3.82	151.9	2.19
74% I6	132.2	46.21	139.0	28.29	144.0	3.99	157.9	2.96
90% I6	127.0	40.25	140.8	31.88	145.6	3.89	168.4	3.10
100% I6	121.0	41.40	150.0	35.44	-	-	171.0	3.72
%Compound (System I8/I16)	$T_{\text{Cr-SmB}}$	$\Delta H_{\text{Cr-SmB}}$	$T_{\text{SmB-SmC}}$	$\Delta H_{\text{SmB-SmC}}$	$T_{\text{SmC-SmA}}$	$\Delta H_{\text{SmC-SmA}}$	$T_{\text{SmA-I}}$	$\Delta H_{\text{SmA-I}}$
0% I8	132.0	44.52	143.0	37.11	-	-	166.0	3.29
25% I8	134.0	39.10	144.0	32.78	153.0	4.00	160.0	3.66
50% I8	126.4	37.50	140.6	25.90	151.2	3.36	154.0	3.10
75% I8	127.3	46.00	142.0	29.09	150.8	3.71	155.8	3.02
90% I8	127.3	42.27	145.5	30.80	151.9	4.16	161.5	3.57
100% I8	113.0	40.49	146.0	31.64	-	-	168.0	3.84

Cr-SmB = solid to the SmB phase transition; SmB-SmC = SmB to the SmC transition; SmC-SmA = SmC to the SmA transition; and SmA-I = SmA to the isotropic phase transition.

**Figure 1.** Binary phase diagrams for (a) system I6/I8; (b) system I6/I16; (c) system I8/I16.

For the binary system **I6/I8**, all mixtures exhibited enantiotropic LC phases, as seen in Table 1. Furthermore, each of them only displayed the same type of mesophase with LC phase at various temperatures, except for 50 and 75 mole % of **I6/I8** mixtures which possessed an induced new phase, with the thermal stability varying according to the length of the terminal alkoxy substituent. Additionally, under crossed polarizers, a typical image was observed for SmC phases exhibited by conventional rod-like LCs mixtures at 50 and 75 mol% of **I6**. The same trend occurred for the binary system **I6/I16**; all mixtures exhibited enantiotropic LC phases and displayed the same mesophase type at various temperatures. However, for 50, 74 and 90 mol% of **I6/I16** mixtures, they observed induced SmC phases. In the final binary system **I8/I16**, the induced SmC phases covered all the binary phase compositions.

2.1.1. Binary Mesophase Thermal Behavior of **I6/I8** Derivatives

Figure 1a shows the binary mixtures of 4-biphenyle-4'-hexyloxybenzenamine (**I6**) with its corresponding homologue 4-biphenyle-4'-octyloxybenzenamine (**I8**), where the mixtures are formed from one lower homologue **I6** and higher homologue **I8**. Both components are dimorphic exhibited SmB and SmA phases with different thermal mesophase stability. As can be seen from Figure 1a, the addition of **I6** component to **I8**, both bearing dissimilar alkoxy chain length, resulted in an increment in the melting temperature, covering all composition ranges of **I6**. Moreover, the SmB-mesophase of all binary mixtures gradually varies with composition, while the SmA-I temperatures virtually linearly depend on composition. This pattern suggests that the molecular arrangements between the two components being mixed are unaffected by the addition of **I6** to **I8**. On the other hand, the addition of nearly 25 mol% of **I6** to **I8** resulted in an appearance of induced SmC phase until approximately the addition of 90 mol% of **I6**. No eutectic mixture of this system has been observed, while the 1:1 mol% of the mixture (50 mol% of **I6**) exhibits a wide mesomorphic temperature range, 31.2 °C. The DSC thermograms of 50 mol% of **I6/I8** are presented in Figure 2, as an example. POM textures of observed mesophases are depicted in Figure 3.

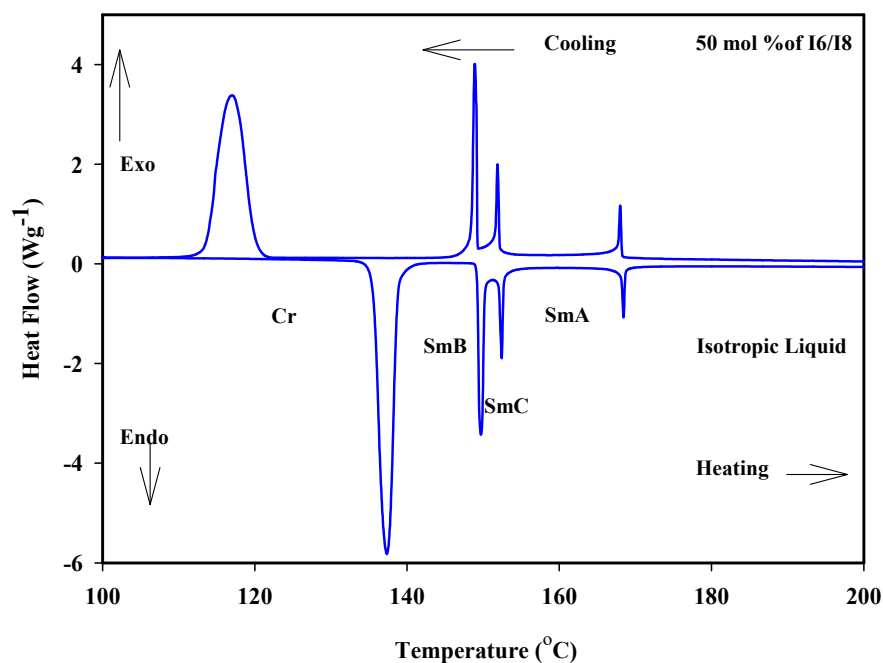


Figure 2. DSC thermogram for 50 mol% **I6/I8** binary system during heating and cooling states at rate 10 °C min^{−1}.



Figure 3. POM textures of 50 mol% of **I6/I8** during heating (a) SmB phase at 142 °C; (b) SmC phase at 150 °C; and (c) SmA phase at 158 °C.

2.1.2. Binary Mesophase Thermal Behavior of **I6/I16** Derivatives

Similarly, the binary phase diagram of the 4-biphenyle-4'-hexyloxybenzenamine (**I6**) and 4-biphenyle-4'-hexadecyloxybenzenamine (**I16**) is illustrated graphically in Figure 1b. As can be seen from Figure 1b, the binary mixture (**I6/I16**) exhibits gradual variation with composition of the crystal–SmB transitions and nearly negative deviation composition dependence of the SmB phase temperatures. This behavior indicates that the introduction of the different proportionated terminal chain length derivatives in the mixture slightly affects the molecular arrangements between the two components being mixed. Furthermore, the two homologous **I6** and **I16** had different sizes, suggesting that they would be placed in an opposite-directed structure; as a result, it is probable that the addition of the higher-length derivative **I16** affects the way the compound **I6**'s molecules are arranged. When the two components are mixed, the SmA stability of both components is frequently impacted and was observed at first drop and then increased with the mol% of **I6**. A good induced SmC mesomorphic range encompassed the mixture's whole composition range starting at 24 mol% **I6**. The DSC thermograms of the 50 mol% of **I6/I16** are presented in Figure 4 as an example.

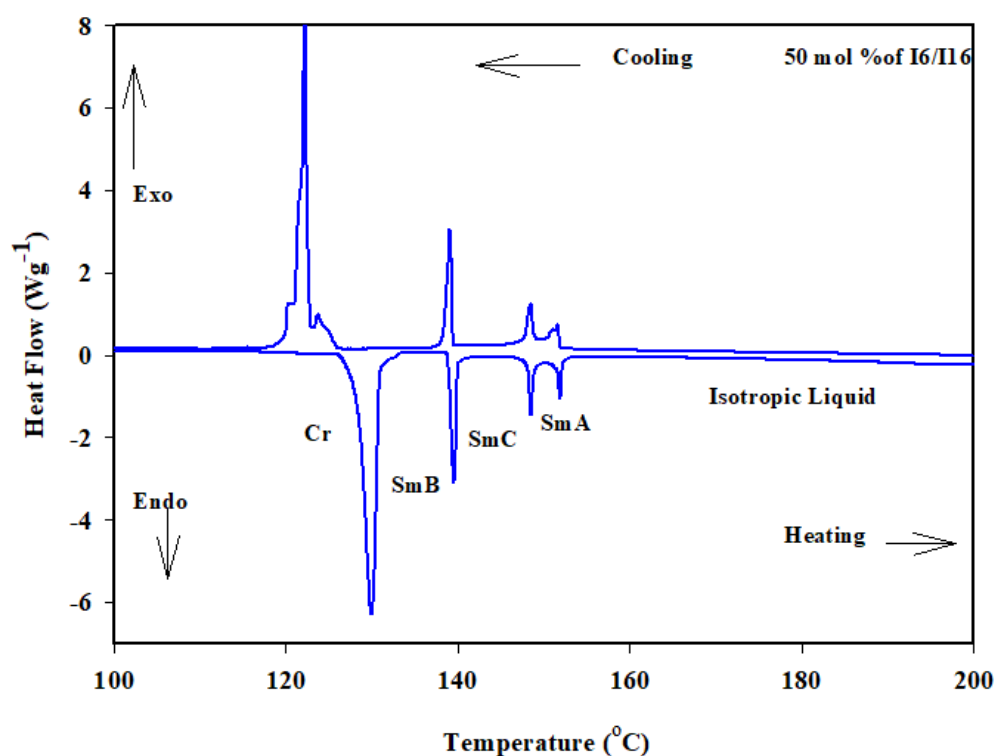


Figure 4. DSC thermogram for 50 mol% **I6/I16** binary system during heating and cooling states at rate 10 °C min^{−1}.

2.1.3. Binary Mesophase Thermal Behavior of I8/I16 Derivatives

Similar behavior was observed for binary mixture of homologues of I8/I16 (Figure 1c), while the induced SmC mesophase covered all composition ranges of the I8 component. It can be also deduced when comparing all phase diagrams that the mesomorphic thermal stability decreases as the alkoxy chain length increases. The DSC thermograms of the 50 mol% of I8/I16 are presented in Figure 5 as an example.

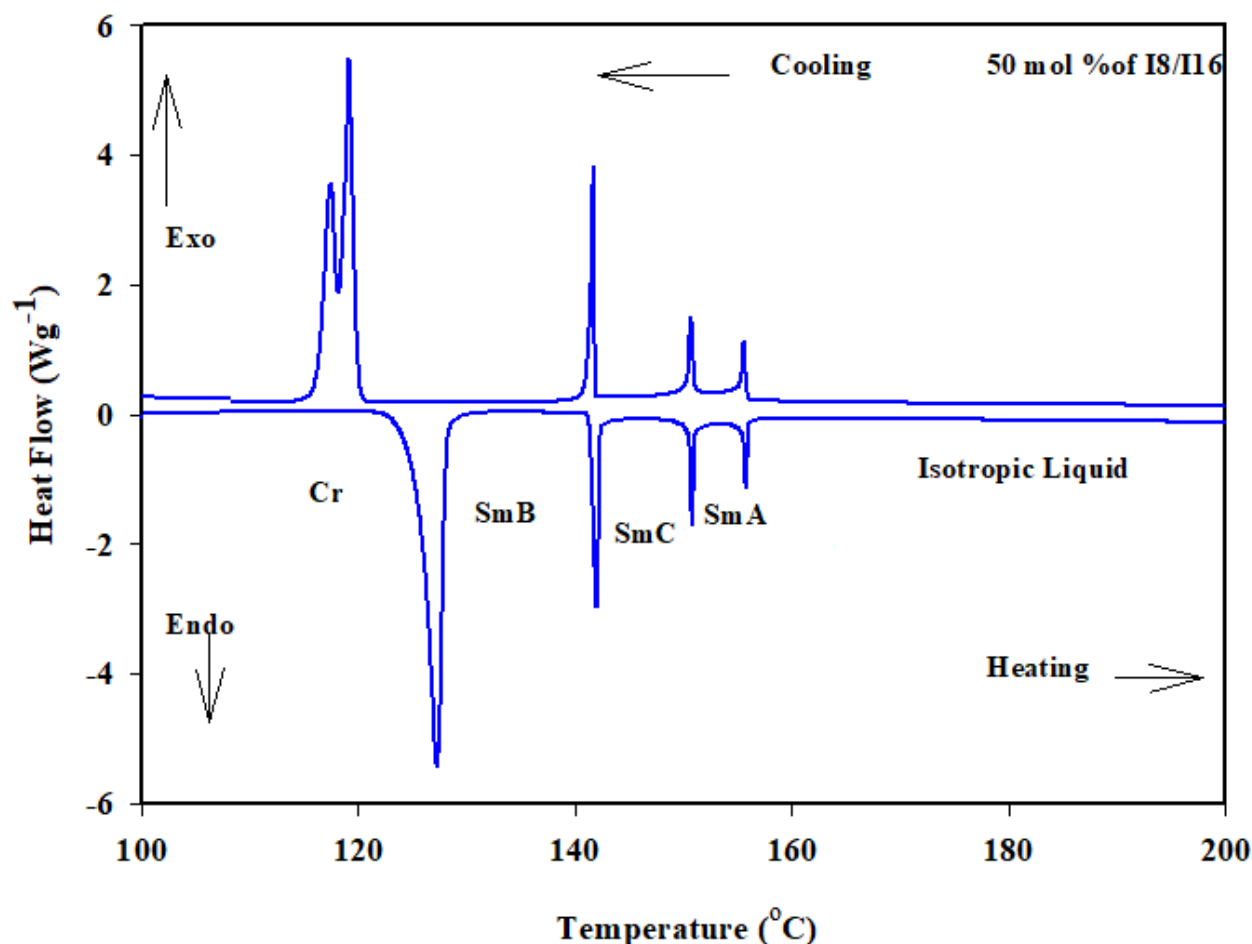


Figure 5. DSC thermogram for 50 mol% I8/I16 binary system during heating and cooling states at rate 10 °C min^{−1}.

To achieve wide temperature ranges for liquid crystalline states, binary systems have frequently been used. If an electron donor–acceptor charge transfer interaction provides the orientational forces in binary mixes of electron donors and acceptors, parallel molecular arrangement, which is necessary for the formation of liquid crystals, becomes evident [67,68]. Park et al. [67] examined the nematic-to-isotropic liquid transition temperature (T_{N-I}) in the binary system of N-(4-methoxybenzylidene)-4'-butylaniline and 4-cyano-4'-pentylbiphenyl, whereby a weak charge transfer interaction occurs between the donor and the acceptor. In this case, although both components exhibit the nematic phase, the composition dependence of T_{N-I} is proved to show a broad curve, whose maximum is located near 1:1 molar ratio, and T_{N-I} higher than that estimated from the straight line joining the T_{N-I} of both components.

Sometimes, in binary mixtures of donors and acceptors, even if both components are non-mesomorphic, their mixture is shown to be potentially mesomorphic. This was achieved by Araya and Matsunaga [68], who observed nematic phase in the binary mixtures of potentially mesomorphic electron donors and acceptors of type N-(4-X-benzylidene)-4'-

Y-aniline. It acts as a donor if X or Y is dimethyl amino group and as an acceptor if X or Y is nitro group.

The production of mixed mesomorphism by combining compounds where none, one, or both are mesogens has been proposed by another study [69]. A considerable amount of focus has been given to the mesophase's emergence [70], changes in mixed mesomorphic ranges and thermal stabilities, and research into the variables that affect modifications.

Cases of liquid crystallinity in mixtures of two non-mesomorphic components have also been reported. For example, Młodziejowski [71] claims that mixtures of cholesterol and acetyl alcohol and of cholesterol and glycerol yield mesomorphic phases and, earlier, Gaubert [72] obtained mesomorphic systems by mixing molten cholesterol with succinimide and with either malic, maleic, malonic, succinic, anisic, cinnamic, or lactic acids. Gaubert also examined the liquid crystalline mixtures obtained by heating ergosteryl acetate, propionate, or butyrate with glycolic acid, with glycerol, and with orcin, and the mesomorphic mixtures obtained on melting certain cholesterol and ergosterol derivatives with urea. Kravchenko and Pastukhova [73] have also reported mesomorphic properties for mixtures of non-mesomorphic compounds such as the hydrocarbons, indene, and naphthalene.

By comparing the mesophase behavior of four binary systems made up of structurally related mesogens and a nematogen containing terminal group, Dave et al. [74] investigated the impact of mixed mesomorphism that results from these variations. The mesomorphic azo and esters derivative made up the binary mixes under investigation.

The analysis of these binary systems revealed that N-I, SmA-N, and SmA-I curves depart from linearity as the molecular geometry of the two components in the binary mixture changes. This non-linear tendency can be caused by various moieties comprising the central bridges and terminal groups. Some researchers have reported on the nonlinear behavior of binary phase diagrams where one of the components includes a strong polar end group [75–77]. The great propensity of the nitro group to facilitate the production of orientated fluids in these binary systems was identified as the cause of the deviation from linearity.

In a study to investigate the effect of molecular length on the mesophase behavior of some liquid crystalline compounds and their binary mixtures, Saad and Nessim [78] examined new model compounds in order to investigate the effect of the terminal chain length on the liquid crystalline phase stability in their pure states and their binary mixtures with each other as well as with their nitro analogue. In the investigated range (C_{12} – C_{20}), no pronounced differences were observed either in the mode of phase behavior or in the mesophase stability of the eutectic mixtures. The only effect observed was in the eutectic compositions, which vary according to the differences in the length of the chain attached to both components of the mixture. Since, the stability of the liquid crystalline molecule increases upon introducing an extra benzene ring (biphenyl moiety) to the molecular structure.

The mesogenic properties of biphenyl groups have been utilized to create liquid crystalline materials with nematic, smectic, and cholesteric phases [75,76]. Furthermore, π - π stacking interactions can be used to interact between biphenyl moieties. Self-assembled monolayers and molecular recognition research have all benefited from the use of these π - π stacking interactions. [77–79]. Prior studies suggest that molecules with biphenyl rings bind with high affinity for molecular recognition as a result of the existence of aromatic domains that result in strong π - π stacking interactions [79,80]. The interactions between biphenyl molecules can be observed as well.

2.2. Absorbance Spectra

The absorbance spectra of 4-Biphenyl-4'-alkyloxybenzenamine and their mixtures are shown in Figure 6. The absorbance spectra show that the synthesized liquid crystal materials absorbed in the UV region and absorbance reduced to zero for the wavelength higher than 400 nm. These samples exhibit a peak at approximately 240 nm that corresponds

to the $\pi \rightarrow \pi^*$ transition in the benzene ring [81,82] and a shoulder at 340 nm. It can be noticed that the mixed liquid crystalline material has slightly higher absorbance as compared with pure materials. The energy bandgap of these materials was evaluated from the extrapolation of Tauc's plot to the energy axis, as shown in Figure 7 [83–85], and the corresponding bandgaps are listed in Table 2. The bandgap of sample **I6** was evaluated to be 3.24 eV and slightly increases with the increase in the alkyl side chain with a bandgap of 3.31 eV and 3.37 eV for **I8** and **I16** samples, respectively. The bandgap of mixed liquid crystalline samples was found to be further increased to 3.48 eV, 3.54 eV, and 3.55 eV for **I6/8**, **I6/16**, and **I8/16**, respectively. The increase in bandgap with the increase in alkyl side-chain length is associated with the increase in steric hindrance in longer-chain-based LC materials. Moreover, in mixed liquid crystalline samples, the steric hindrance further increase as a result of the further increase in band gap.

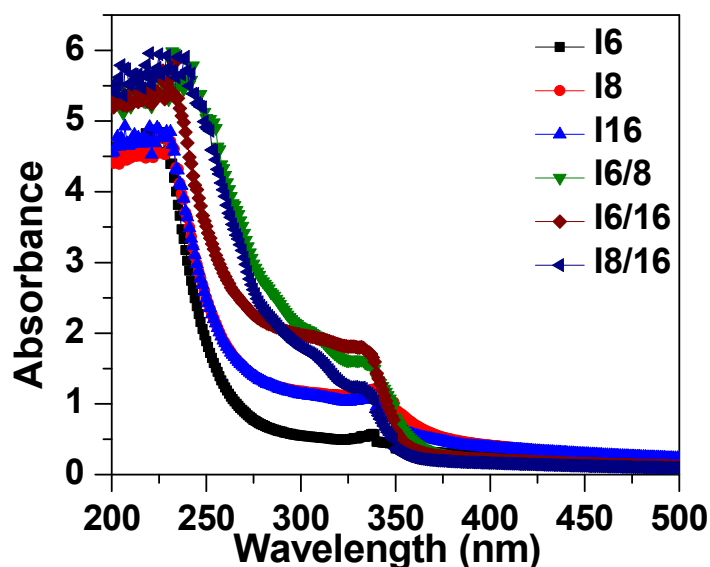


Figure 6. Absorption spectra of investigated materials **I_n** and their binary mixtures.

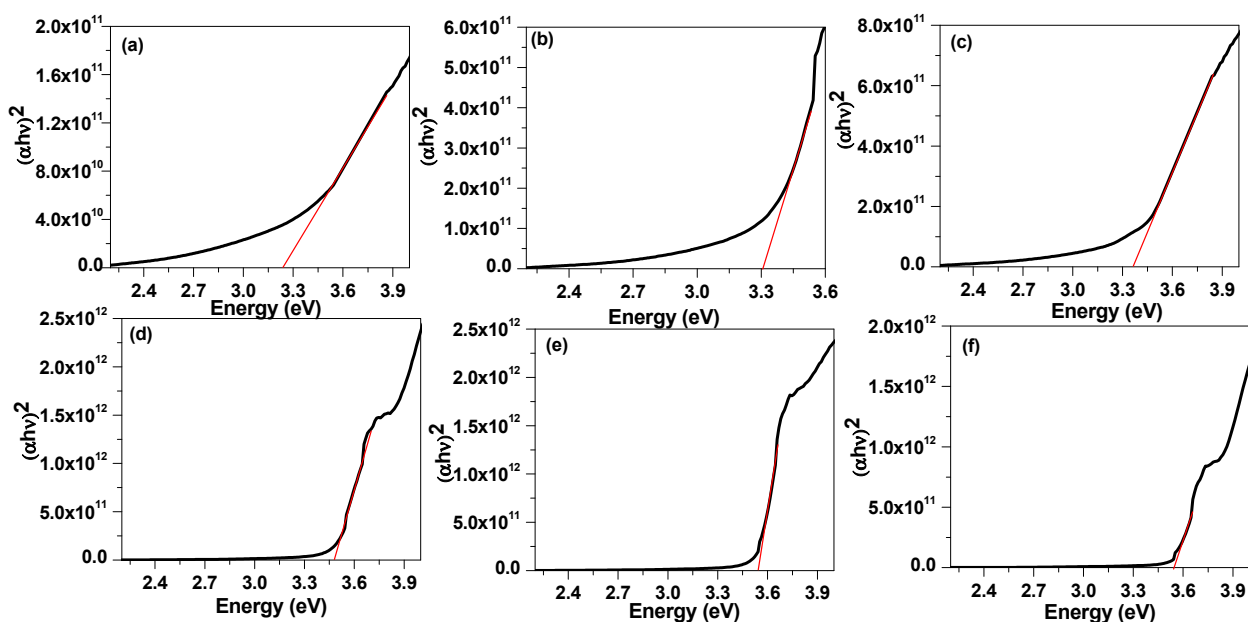
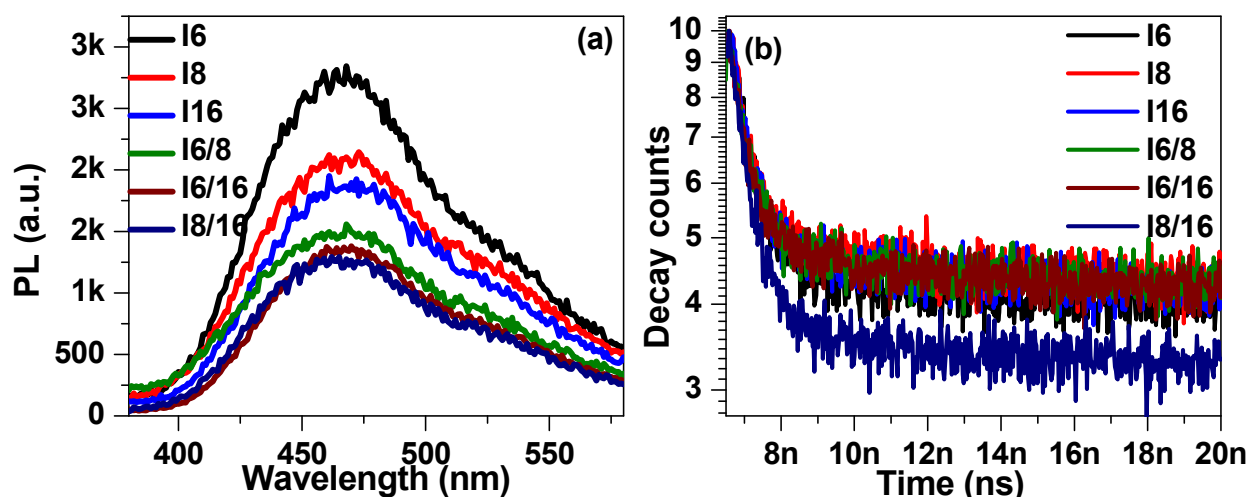


Figure 7. Tauc Plot (black line) of (a) **I6**, (b) **I8**, (c) **I16**, (d) **I6/8**, (e) **I6/16** and (f) **I8/16**. The evaluation of band gap was carried out from the intercept of tangent (red line) on energy axis.

Table 2. The optical parameters evaluated from absorbance and fitting of time-resolved fluorescence spectra.

Sample	E _g (eV)	A	τ (ps)	χ ²
I6	3.24	434	665	1.15
I8	3.31	464	638	1.21
I16	3.37	444	629	0.98
I6/8	3.48	456	600	0.92
I6/16	3.54	464	513	0.99
I8/16	3.55	351	582	0.94

The steady-state fluorescence spectra of 4-Biphenyle-4'-alkyloxybenzenamine based liquid crystalline materials in pure and mixed states are shown in Figure 8a. The steady-state spectra were recorded by exciting the samples by a laser diode of 319 nm ± 10 nm. The steady-state spectra show a broad emission between 400 nm to 580 nm with maxima at approximately 465 nm, and no significant shift in the peak position was noticed for any sample. The photoluminescence (PL) intensity was found to be quenched with the increase in alkyl chain length. This might be attributed to the creation of defect states where charge carrier gets trapped before returning to the ground state. The time-resolved fluorescence decay spectra of synthesized liquid crystalline materials were recorded at 465 nm and the results are illustrated in Figure 8b. The decay spectra were fitted with a single exponential decay function [86–89]: $I(t) = A + Be^{-t/\tau}$, where τ is the lifetime and A and B are fitting constants. The lifetime of I6 sample was extracted to be 533 ps and found to be slightly increased with the increase in alkyl group length. The lifetime of I8 and I16 were evaluated to be 629 ps and 638 ps, respectively. The decrease in lifetime ascribes to the trapping of charge carriers in trap states associated with the increase in alkyl group length in 4-Biphenyle-4'-alkyloxybenzenamine-based liquid crystalline materials. Moreover, the defect states in the mixed LC samples further increase as a result of the further drop in PL intensity and, consequently, the decrease in charge carrier lifetime, as evident from Figure 8a,b.

**Figure 8.** The steady-state (a) and time-resolved (b) PL spectra of investigated materials **I_n** in pure and mixed states.

2.3. Experimental

The compounds used in this investigation were prepared and characterized according to earlier descriptions [66].

2.4. Instrumentation

A Q20 Differential Scanning Calorimeter from TA Instruments Co. was used to conduct the calorimetric experiments (DSC; Des Plaines, IL, USA). Utilizing the melting point and enthalpy of indium and lead, the DSC was calibrated. DSC analysis was carried out on little samples (2–3 mg) that were deposited in aluminum pans. In an inert atmosphere of nitrogen gas, all measurements were made at a heating rate of 10 °C/min, with all transitions being recorded from the second heating scan.

Using a common polarized optical microscope (POM, Wild, Germany) connected to a homemade hot stage, transition temperatures were verified and the type of mesophase identified for all products synthesized.

In order to prepare binary mixtures, carefully weighed samples of the required amounts of each individual component ($\pm 1.0\%$ in composition) were mixed, melted to create an intimate mixture, and then cooled to room temperature while being stirred. The absorption spectra of liquid crystalline samples were recorded on glass slides using an Agilent Cary 5000 UV-Vis-NIR spectrophotometer. The steady-state fluorescence spectra and time-resolved decay spectra were recorded by DeltaFlex time-correlated single photon counting (TCSPC) system from Horiba. To measure the emission spectra, samples were excited by a Delta-diode laser of peak wavelength $\lambda \sim 320 \pm 10$ nm, whereas the decay spectra were recorded for $\lambda = 465$ nm.

3. Conclusions

A series of biphenyl liquid crystal homologues were constructed and their mesophase and optical behavior were investigated for energy investigations in pure and mixed states. Depending on their side-chain length, all individual materials show dimorphic SmB and SmA mesophases enantiotropically with varying thermal stabilities. In order to better understand how mixing liquid crystalline molecules with various terminal alkoxy chain lengths affects the mesomorphic and optical properties of the mixtures, the current investigation was carried out. Intimate blends were produced by mixing compounds of various sizes bearing different terminal alkoxy side chains. Binary mixtures demonstrated that the stacking interactions between the biphenyl rings in the mixture improve the mesomorphic characteristics and result in an induced SmC phase. The energy bandgap was found to increase with the increments of alkyl side-chain length and further increases in mixed LC samples. The PL intensity quenched for longer alkyl side-chain length-based LC and further decreased in mixed samples. Moreover, the longer alkyl side-chain length and mixing of two LC materials create the steric hindrance and defect states which results in the faster decay of charge carriers.

Supplementary Materials: The following supporting information can be downloaded at: <https://www.mdpi.com/article/10.3390/cryst13040645/s1>. S1: The information of characterization analyses of derivatives In.

Author Contributions: Conceptualization, M.T.K.; Methodology, S.A.A.-Z., N.M., Y.A.J. and H.A.A.; Validation, V.J.; Formal analysis, S.A.A.-Z., M.T.K., Y.A.J., F.M.A. and H.A.A.; Investigation, V.J., N.M. and H.A.A.; Resources, S.A.A.-Z., M.T.K. and V.J.; Data curation, N.M.; Writing—original draft, S.A.A.-Z., V.J. and Y.A.J.; Writing—review & editing, S.A.A.-Z., M.T.K., N.M., H.A.A. and F.M.A.; Visualization, Y.A.J.; Funding acquisition, S.A.A.-Z. All authors have read and agreed to the published version of the manuscript.

Funding: This research was funded by Scientific Research Deanship at University of Ha'il, Saudi Arabia, through project number RG-21018.

Data Availability Statement: The data used for research described in this manuscript are available upon request from corresponding author: ahoda@sci.cu.edu.eg.

Conflicts of Interest: The authors declare no conflict of interest.

References

1. Veerabhadraswamy, B.N.; Rao, D.S.S.; Yelamagad, C.V. Ferroelectric Liquid Crystals: Synthesis and Thermal Behavior of Optically Active, Three-Ring Schiff Bases and Salicylaldehydes. *Chem. Asian J.* **2018**, *13*, 1012–1023. [\[CrossRef\]](#) [\[PubMed\]](#)
2. Huang, C.-C.; Hsu, C.-C.; Chen, L.-W.; Cheng, Y.-L. The effect of position of (S)-2-octyloxy tail on the formation of frustrated blue phase and antiferroelectric phase in Schiff base liquid crystals. *Soft Matter* **2014**, *10*, 9343–9351. [\[CrossRef\]](#) [\[PubMed\]](#)
3. Segura, J.L.; Mancheño, M.J.; Zamora, F. Covalent organic frameworks based on Schiff-base chemistry: Synthesis, properties and potential applications. *Chem. Soc. Rev.* **2016**, *45*, 5635–5671. [\[CrossRef\]](#) [\[PubMed\]](#)
4. Gowda, A.; Jacob, L.; Joy, N.; Philip, R.; Pratibha, R.; Kumar, S. Thermal and nonlinear optical studies of newly synthesized EDOT based bent-core and hockey-stick like liquid crystals. *New J. Chem.* **2018**, *42*, 2047–2057. [\[CrossRef\]](#)
5. Hagar, M.; Ahmed, H.A.; Saad, G.R. Mesophase stability of new Schiff base ester liquid crystals with different polar substituents. *Liq. Cryst.* **2018**, *45*, 1324–1332. [\[CrossRef\]](#)
6. Alamro, F.S.; Gomha, S.M.; Shaban, M.; Altowyan, A.S.; Abolibda, T.Z.; Ahmed, H.A. Optical investigations and photoactive solar energy applications of new synthesized Schiff base liquid crystal derivatives. *Sci. Rep.* **2021**, *11*, 15046. [\[CrossRef\]](#)
7. Gomha, S.; Ahmed, H.; Shaban, M.; Abolibda, T.; Khushaim, M.; Alharbi, K. Synthesis, Optical Characterizations and Solar Energy Applications of New Schiff Base Materials. *Materials* **2021**, *14*, 3718. [\[CrossRef\]](#)
8. Al-Mutabagani, L.A.; Alshabanah, L.A.; Gomha, S.M.; Abolibda, T.Z.; Shaban, M.; Ahmed, H.A. Synthesis and Mesomorphic and Electrical Investigations of New Furan Liquid Crystal Derivatives. *Front. Chem.* **2021**, *9*, 711862. [\[CrossRef\]](#)
9. Khan, M.T. Unraveling the impact of graphene nanostructures passivation on the electrical properties of the perovskite solar cell. *Mater. Sci. Semicond. Process.* **2023**, *153*, 107172. [\[CrossRef\]](#)
10. Alamro, F.S.; Ahmed, H.A.; Gomha, S.M.; Shaban, M. Synthesis, Mesomorphic, and Solar Energy Characterizations of New Non-Symmetrical Schiff Base Systems. *Front. Chem.* **2021**, *9*, 686788. [\[CrossRef\]](#)
11. Georgiev, A.; Stoilova, A.; Dimov, D.; Yordanov, D.; Zhivkov, I.; Weiter, M. Synthesis and photochromic properties of some N-phthalimide azo-azomethine dyes. A DFT quantum mechanical calculations on imine-enamine tautomerism and trans-cis photoisomerization. *Spectrochim. Acta Part A Mol. Biomol. Spectrosc.* **2019**, *210*, 230–244. [\[CrossRef\]](#) [\[PubMed\]](#)
12. Ovdenko, V.; Kolendo, A. New bent-shaped azomethine monomers for optical applications. *Mol. Cryst. Liq. Cryst.* **2016**, *640*, 113–121. [\[CrossRef\]](#)
13. Komissarova, O.A.; Lukyanov, B.S.; Lukyanova, M.B.; Ozhogin, I.V.; Mukhanov, E.L.; Korobov, M.S.; Rostovtseva, I.A.; Minkin, V.I. New indoline spiropyrans containing azomethine fragment. *Russ. Chem. Bull.* **2017**, *66*, 2122–2125. [\[CrossRef\]](#)
14. Stoilova, A.; Georgiev, A.; Nedelchev, L.; Nazarova, D.; Dimov, D. Structure-property relationship and photoinduced birefringence of the azo and azo-azomethine dyes thin films in PMMA matrix. *Opt. Mater.* **2019**, *87*, 16–23. [\[CrossRef\]](#)
15. Georgiev, A.; Kostadinov, A.; Ivanov, D.; Dimov, D.; Stoyanov, S.; Nedelchev, L.; Nazarova, D.; Yancheva, D. Synthesis, spectroscopic and TD-DFT quantum mechanical study of azo-azomethine dyes. A laser induced trans-cis-trans photoisomerization cycle. *Spectrochim. Acta Part A Mol. Biomol. Spectrosc.* **2018**, *192*, 263–274. [\[CrossRef\]](#)
16. Reddy, D.S.; Reddy, G.S.; Beatriz, A.; Corey, E.J. Contrasting Diastereoselectivity between Cyclic Nitrones and Azomethine Ylides. Stereocontrolled Pathways to cis-anti-anti-cis-Oxazetetrakinanes from a Bicyclic Nitron. *Org. Lett.* **2021**, *23*, 5445–5447. [\[CrossRef\]](#)
17. Ruslim, C.; Ichimura, K.J. Z-Isomers of 3,3'-disubstituted azobenzenes highly compatible with liquid crystals. *Mater. Chem.* **1999**, *9*, 673–681. [\[CrossRef\]](#)
18. Ichimura, K. Photoalignment of Liquid-Crystal Systems. *Chem. Rev.* **2000**, *100*, 1847–1874. [\[CrossRef\]](#)
19. Ikeda, T. Photomodulation of liquid crystal orientations for photonic applications. *J. Mater. Chem.* **2003**, *13*, 2037–2057. [\[CrossRef\]](#)
20. Naoum, M.M.; Fahmi, A.A.; Alaasar, M.A. Supramolecular Hydrogen-Bonded Liquid Crystals Formed from 4-(4'-Pyridylazophenyl)-4''-alkoxy Benzoates and 4-Substituted Benzoic Acids. *Mol. Cryst. Liq. Cryst.* **2008**, *487*, 74–91. [\[CrossRef\]](#)
21. Blatch, A.E.; Luckhurst, G.R. The liquid crystal properties of symmetric and non-symmetric dimmers based on the azobenzene mesogenic group. *Liq. Cryst.* **2000**, *27*, 775–787. [\[CrossRef\]](#)
22. Thaker, B.; Kanojiya, J. Mesomorphic properties of liquid crystalline compounds with biphenyl moiety containing azo-ester, azo-cinnamate central linkages and different terminal group. *Liq. Cryst.* **2011**, *38*, 1035–1055. [\[CrossRef\]](#)
23. Alaasar, M. Azobenzene-containing bent-core liquid crystals: An overview. *Liq. Cryst.* **2016**, *43*, 2208–2243. [\[CrossRef\]](#)
24. Niezgoda, I.; Jaworska, J.; Pocięcha, D.; Galewski, Z. The kinetics of the E-Z-E isomerisation and liquid-crystalline properties of selected azobenzene derivatives investigated by the prism of the ester group inversion. *Liq. Cryst.* **2015**, *42*, 1148–1158. [\[CrossRef\]](#)
25. Hegde, G.; Shanker, G.; Gan, S.M.; Yuvaraj, A.R.; Mahmood, S.; Mandal, U.K. Synthesis and liquid crystalline behaviour of substituted (E)-phenyl-4-(phenyldiazenyl) benzoate derivatives and their photo switching ability. *Liq. Cryst.* **2016**, *43*, 1578–1588. [\[CrossRef\]](#)
26. Paterson, D.A.; Xiang, J.; Singh, G.; Walker, R.; Agra-Kooijman, D.M.; Martinez-Felipe, A.; Gan, M.; Storey, J.M.D.; Kumar, S.; Lavrentovich, O.D.; et al. Reversible Isothermal Twist-Bend Nematic-Nematic Phase Transition Driven by the Photoisomerization of an Azobenzene-Based Nonsymmetric Liquid Crystal Dimer. *J. Am. Chem. Soc.* **2016**, *138*, 5283–5289. [\[CrossRef\]](#)
27. Romero-Hasler, P.; Fierro-Armijo, A.E.; Soto-Bustamante, E.A.; Meneses-Franco, A. Synthesis and characterisation of two homologous series of LC acrylic monomers based on phenolic and resorcinic azobenzene groups. *Liq. Cryst.* **2016**, *43*, 1804–1812. [\[CrossRef\]](#)

28. Henderson, P.; Cook, A.; Imrie, C. Oligomeric liquid crystals: From monomers to trimers. *Liq. Cryst.* **2004**, *31*, 1427–1434. [\[CrossRef\]](#)
29. Osman, F.; Yeap, G.-Y.; Nagashima, A.; Ito, M.M. Structure property and mesomorphic behaviour of S-shaped liquid crystal oligomers possessing two azobenzene moieties. *Liq. Cryst.* **2016**, *43*, 1283–1292. [\[CrossRef\]](#)
30. Srinivasa, H.T. New symmetric azobenzene molecules of varied central cores: Synthesis and characterisation for liquid crystalline properties. *Liq. Cryst.* **2017**, *44*, 1384–1393. [\[CrossRef\]](#)
31. Rochon, P.; Batalla, E.; Natansohn, A. Optically induced surface gratings on azoaromatic polymer films. *Appl. Phys. Lett.* **1995**, *66*, 136–138. [\[CrossRef\]](#)
32. Wang, M.; Guo, L.X.; Lin, B.P.; Zhang, X.Q.; Sun, Y.; Yang, H. Photo-responsive polysiloxane-based azobenzene liquid crystalline polymers prepared by thiol-ene click chemistry. *Liq. Cryst.* **2016**, *43*, 1626–1635. [\[CrossRef\]](#)
33. Goodby, J.W.; Mandle, J.; Davis, J.; Zhong, C.; Cowling, J. What makes a liquid crystal? The effect of free volume on soft matter. *Liq. Cryst.* **2015**, *42*, 593–622. [\[CrossRef\]](#)
34. Hagar, M.; Ahmed, H.; Saad, G. Synthesis and mesophase behaviour of Schiff base/ester 4-(arylideneamino)phenyl-4''-alkoxy benzoates and their binary mixtures. *J. Mol. Liq.* **2019**, *273*, 266–273. [\[CrossRef\]](#)
35. Ahmed, H.A.; Hagar, M.; Saad, G. Impact of the proportionation of dialkoxy chain length on the mesophase behaviour of Schiff base/ester liquid crystals; experimental and theoretical study. *Liq. Cryst.* **2019**, *46*, 1611–1620. [\[CrossRef\]](#)
36. Hagar, M.; Ahmed, H.A.; Alhaddad, O.A. New azobenzene-based natural fatty acid liquid crystals with low melting point: Synthesis, DFT calculations and binary mixtures. *Liq. Cryst.* **2019**, *46*, 2223–2234. [\[CrossRef\]](#)
37. Hagar, M.; Ahmed, H.; Saad, G. New calamitic thermotropic liquid crystals of 2-hydroxypyridine ester mesogenic core: Mesophase behaviour and DFT calculations. *Liq. Cryst.* **2019**, *47*, 114–124. [\[CrossRef\]](#)
38. Ahmed, H.A.; Hagar, M.; Alaasar, M.; Naoum, M. Wide nematic phases induced by hydrogen-bonding. *Liq. Cryst.* **2019**, *46*, 550–559. [\[CrossRef\]](#)
39. Ahmed, H.; Hagar, M.; Alhaddad, O. Mesomorphic and geometrical orientation study of the relative position of fluorine atom in some thermotropic liquid crystal systems. *Liq. Cryst.* **2019**, *47*, 404–413. [\[CrossRef\]](#)
40. Ahmed, H.A.; Hagar, M.; El-Sayed, T.H.; Alnoman, R.B. Schiff base/ester liquid crystals with different lateral substituents: Mesophase behaviour and DFT calculations. *Liq. Cryst.* **2019**, *46*, 1–11. [\[CrossRef\]](#)
41. Omar, A.Z.; El-Atawy, M.A.; Alsubaie, M.S.; Alazmi, M.L.; Ahmed, H.A.; Hamed, E.A. Synthesis and Computational Investigations of New Thioether/Azomethine Liquid Crystal Derivatives. *Crystals* **2023**, *13*, 378. [\[CrossRef\]](#)
42. Ahmed, H.A.; Hagar, M.; Alhaddad, O.A. New chair shaped supramolecular complexes-based aryl nicotinate derivative; mesomorphic properties and DFT molecular geometry. *RSC Adv.* **2019**, *9*, 16366–16374. [\[CrossRef\]](#) [\[PubMed\]](#)
43. Nafee, S.S.; Hagar, M.; Ahmed, H.A.; Alhaddad, O.; El-Shishtawy, R.M.; Raffah, B.M. New two rings Schiff base liquid crystals; ball mill synthesis, mesomorphic, Hammett and DFT studies. *J. Mol. Liq.* **2019**, *299*, 112161. [\[CrossRef\]](#)
44. Al-Zahrani, S.A.; Khan, M.T.; Jevtovic, V.; Masood, N.; Jeilani, Y.A.; Ahmed, H.A. Design of Liquid Crystal Materials Based on Palmitate, Oleate, and Linoleate Derivatives for Optoelectronic Applications. *Molecules* **2023**, *28*, 1744. [\[CrossRef\]](#) [\[PubMed\]](#)
45. Alhaddad, O.A.; Khushaim, M.S.; Gomha, S.M.; Ahmed, H.A.; Naoum, M.M. Mesophase behavior of four ring ester/azomethine/ester liquid crystals in pure and mixed states. *Liq. Cryst.* **2022**, *49*, 1395–1402. [\[CrossRef\]](#)
46. O'Neill, M.; Kelly, S. Liquid Crystals for Charge Transport, Luminescence, and Photonics. *Adv. Mater.* **2003**, *15*, 1135–1146. [\[CrossRef\]](#)
47. Andrienko, D. Introduction to liquid crystals. *J. Mol. Liq.* **2018**, *267*, 520–541. [\[CrossRef\]](#)
48. Jaishi, B.R.; Mandal, P.K.; Dabrowski, R. Studies on binary mixtures of 4-pentyloxy-4'-cyanobiphenyl. *Opto-Electron. Rev.* **2010**, *18*, 111–120. [\[CrossRef\]](#)
49. Manohar, R.; Srivastava, A.K.; Jyotishman, P.; Shukla, J.P.; Prajapati, A.K.; Bonde, N.L. Dielectric, optical and thermodynamical properties of liquid crystal sample exhibiting sm a phase. *Int. J. Phys. Sci.* **2006**, *1*, 147–153.
50. Kim, N.; Huang, T.M.; Kyu, T.; Nosaka, M.; Kudo, H.; Nishikubo, T. Induced smectic phase in mixtures of hyper branch polyester and liquid crystal mesogens. *J. Phys. Chem.* **2008**, *112*, 13225–13230. [\[CrossRef\]](#)
51. Govindaiah, T.; Sreepad, H. Phase transition and thermal characterization of induced smectic phases in a ternary mixture. *J. Mol. Liq.* **2015**, *202*, 75–78. [\[CrossRef\]](#)
52. Diele, S.; Pelzl, G.; Weissflog, W.; Demus, D. A filled smectic A phase A novel kind of induced smectic A phase observed for binary mixtures. *Liq. Cryst.* **1988**, *3*, 1047–1053. [\[CrossRef\]](#)
53. Sadowska, K.W.; Zywockinski, A.; Stecki, J.; Dabrowski, R. Induced smectic phases, densities of binary mixtures of 4, 4'-dialkylazoxybenzenes with 4-pentyl-4'-cyanobiphenyl (PCB). *J. Phys.* **1982**, *43*, 1673–1678. [\[CrossRef\]](#)
54. Oh, C.S. Induced Smectic Mesomorphism by Incompatible Nematogens. *Mol. Cryst. Liq. Cryst.* **1977**, *42*, 1–14. [\[CrossRef\]](#)
55. Hwang, J.C.; Kikuchi, H.; Kajiyama, T. Aggregation states and electro-optical properties of the induced smectic phase by mixing a nematic liquid crystalline polymer and a low molecular weight liquid crystal. *Polymer* **1992**, *33*, 1822–1825. [\[CrossRef\]](#)
56. Naoum, M.M.; Fahmi, A.A.; Alaasar, M.A.; Abdel-Aziz, M.E. Effect of lateral substitution of different polarity on the mesophase behavior in pure and mixed states of 4-(4'-substituted phenylazo)-2-substituted phenyl-4''-alkoxy benzoates. *Liq. Cryst.* **2011**, *38*, 391–405. [\[CrossRef\]](#)

57. Alamro, F.S.; Tolan, D.A.; El-Nahas, A.M.; Ahmed, H.A.; El-Atawy, M.A.; Al-Kadhi, N.S.; Aziz, S.G.; Shibl, M.F. Wide Nematogenic Azomethine/Ester Liquid Crystals Based on New Biphenyl Derivatives: Mesomorphic and Computational Studies. *Molecules* **2022**, *27*, 4150. [\[CrossRef\]](#)
58. Imrie, C. Non-symmetric liquid crystal dimers: How to make molecules intercalate. *Liq. Cryst.* **2006**, *33*, 1449–1485. [\[CrossRef\]](#)
59. Ooi, Y.-H.; Yeap, G.-Y.; Han, C.-C.; Lin, H.-C.; Kubo, K.; Ito, M.M. Synthesis and smectogenic properties of novel phloroglucinol-based star-shaped liquid crystals containing three peripheral alkyloxyated Schiff base arms. *Liq. Cryst.* **2013**, *40*, 516–527. [\[CrossRef\]](#)
60. Hinojosa, A.R.C.; de Souza, S.P.; Alves, T.V.; dos Santos, I.T.O.; Silva, E.O.; Gonçalves, I.L.; Merlo, A.A.; Junkes, C.F.; Bechtold, I.H.; Vieira, A.A. Shining rings: The effect of the rigid core and benzazole heterocycles on the properties of luminescent calamitic liquid crystals. *J. Mol. Liq.* **2021**, *338*, 116614. [\[CrossRef\]](#)
61. Alamro, F.; Ahmed, H.; El-Atawy, M.; Al-Zahrani, S.; Omar, A. Induced Nematic Phase of New Synthesized Laterally Fluorinated Azo/Ester Derivatives. *Molecules* **2021**, *26*, 4546. [\[CrossRef\]](#) [\[PubMed\]](#)
62. Alrefae, S.H.; Ahmed, H.A.; Khan, M.T.; Al-Ola, K.A.; Al-Refai, H.; El-Atawy, M.A. New Self-Organizing Optical Materials and Induced Polymorphic Phases of Their Mixtures Targeted for Energy Investigations. *Polymers* **2022**, *14*, 456. [\[CrossRef\]](#)
63. Ahmed, H.A. Thermal behavior of binary mixtures of isomers of different molecular structures and different lateral substituent positions. *J. Therm. Anal. Calorim.* **2016**, *125*, 823–830. [\[CrossRef\]](#)
64. Abberley, J.P.; Jansze, S.M.; Walker, R.; Paterson, D.A.; Henderson, P.A.; Marcelis, A.T.M.; Storey, J.M.D.; Imrie, C.T. Structure–property relationships in twist-bend nematogens: The influence of terminal groups. *Liq. Cryst.* **2017**, *44*, 68–83. [\[CrossRef\]](#)
65. Mohammady, S.Z.; Aldhayan, D.M.; Alshammri, M.A.; Alshammari, A.K.; Alazmi, M.; Katariya, K.D.; Jaremko, M.; Hagar, M. Polar Alkoxy Group and Pyridyl Effects on the Mesomorphic Behavior of New Non-Symmetrical Schiff Base Liquid Crystals. *Symmetry* **2021**, *13*, 1832. [\[CrossRef\]](#)
66. Park, J.W.; Bak, C.S.; Labes, M.M. Effects of molecular complexing on the properties of binary nematic liquid crystal mixtures. *J. Am. Chem. Soc.* **1975**, *97*, 4398–4400. [\[CrossRef\]](#)
67. Araya, K.; Matsunaga, Y. Liquid Crystal Formation in Binary Systems. I. An Interpretation of the Phase Diagrams of the Azoxydianisole–Schiff Base Systems. *Bull. Chem. Soc. Jpn.* **1980**, *53*, 989–993. [\[CrossRef\]](#)
68. Dave, J.S.; Lohar, J.M. Liquid-crystalline characteristics of ester mesogens-para-chlorophenyl para'-normal-alkoxycinnamates. *J. Indian Chem. Soc.* **1989**, *66*, 25–27.
69. Lohar, J.M.; Dave, J.S., Jr. Emergence of smectic mesophase in binary mixtures of pure nematogens. *Mol. Cryst. Liq. Cryst.* **1983**, *103*, 181–192. [\[CrossRef\]](#)
70. Młodziejowski, A. Dissoziation der flüssigen Kristalle. *Z. Phys. Chem.* **1928**, *135*, 129–146. [\[CrossRef\]](#)
71. Gaubert, P. Nouvelle contribution à l'étude des sphérolites (polymorphisme de la codéine, de la thébaine et de la narcotine). *Bull. Minéral.* **1913**, *36*, 45–64. [\[CrossRef\]](#)
72. Kravchenko, V.M.; Pastukhova, I.S. Dvukhkompontnye tverdye rastvory i evtekticheskie sistemy indena, izokhinolina, naftalina i benzola. *Zhurnal Prikl. Khimii* **1952**, *25*, 313–321.
73. Dave, J.S.; Menon, M.R.; Patel, P.R. Synthesis and mesomorphic characteristics of mesogens with branched isoamyloxy and isobutyloxy terminal groups. *Mol. Cryst. Liq. Cryst.* **2002**, *378*, 1–11. [\[CrossRef\]](#)
74. Schroeder, J.P.; Bristol, D.W. Liquid crystals. IV. Effects of terminal substituents on the nematic mesomorphism of p-phenylene dibenzoates. *J. Org. Chem.* **1973**, *38*, 3160–3164. [\[CrossRef\]](#)
75. Park, J.W.; Labes, M.M. Broadening of the nematic temperature range by a non-mesogenic solute in a nematic liquid crystal. *Mol. Cryst. Liq. Cryst.* **1976**, *34*, 147–152. [\[CrossRef\]](#)
76. El-Atawy, M.A.; Omar, A.Z.; Alazmi, M.L.; Alsubaie, M.S.; Hamed, E.A.; Ahmed, H.A. Synthesis and characterization of new imine liquid crystals based on terminal perfluoroalkyl group. *Heliyon* **2023**, *9*, e14871. [\[CrossRef\]](#)
77. Saad, G.R.; Nessim, R.I. Effect of molecular structure on the phase behaviour of some liquid crystalline compounds and their binary mixtures VI [1]. The effect of molecular length. *Liq. Cryst.* **1999**, *26*, 629–636. [\[CrossRef\]](#)
78. Cigl, M.; Hampl, F.; Svoboda, J.; Podoliak, N.; Stulov, S.; Kohout, M.; Novotná, V. Laterally substituted biphenyl benzoates—Synthesis and mesomorphic properties. *Liq. Cryst.* **2021**, *48*, 526–536. [\[CrossRef\]](#)
79. Zhu, S.; Chigan, J.; Li, W.; Yang, J.; Chen, W.; Zhang, W.; Niu, X.; Chen, X.; An, Z.J. The effect of intermolecular actions on the mesomorphic properties of alkenoxy biphenyl-based liquid crystals. *J. Mol. Liq.* **2019**, *296*, 111880. [\[CrossRef\]](#)
80. Yang, R.; Chen, L.; Ruan, C.; Zhong, H.-Y.; Wang, Y.-Z. Chain folding in main-chain liquid crystalline polyesters: From π - π stacking toward shape memory. *J. Mater. Chem. C* **2014**, *2*, 6155. [\[CrossRef\]](#)
81. Liu, G.-F.; Ye, B.-H.; Ling, Y.-H.; Chen, X.-M. Interlocking of molecular rhombi into a 2D polyrotaxane network via π - π interactions. Crystal structure of [Cu 2 (bpa) 2 (phen) 2 (H 2 O)] 2 · 2H 2 O (bpa 2 = biphenyl-4, 4'-dicarboxylate, phen = 1, 10-phenanthroline). *Chem. Commun.* **2002**, *14*, 1442. [\[CrossRef\]](#) [\[PubMed\]](#)
82. Pellequer, J.-L.; Chen, S.W.; Keum, Y.; Karu, A.E.; Li, Q.X.; Roberts, V.A. Structural basis for preferential binding of non-ortho-substituted polychlorinated biphenyls by the monoclonal antibody S2B1. *J. Mol. Recognit.* **2005**, *18*, 282. [\[CrossRef\]](#) [\[PubMed\]](#)
83. Petriello, M.C.; Newsome, B.J.; Dziubla, T.D.; Hilt, J.Z.; Bhattacharyya, D.; Hennig, B. Modulation of persistent organic pollutant toxicity through nutritional intervention: Emerging opportunities in biomedicine and environmental remediation. *Sci. Total Environ.* **2014**, *491–492*, 11–16. [\[CrossRef\]](#) [\[PubMed\]](#)

84. Jacquemin, D.; Laurent, A.D.; Perpète, E.A.; André, J.-M. An ab initio simulation of the UV/visible spectra of *N*-benzylideneaniline dyes. *Int. J. Quantum Chem.* **2009**, *109*, 3506–3515. [[CrossRef](#)]
85. Nozomu, E.; Benzylideneaniline, I. Structure and Ultraviolet Absorption Spectrum of Benzylideneaniline. *Bull. Chem. Soc. Jpn.* **1960**, *33*, 534–539.
86. Khan, M.T.; Almohammed, A.; Shkir, M.; Aboud, S.W. Effect of Ag₂S nanoparticles on optical, photophysical and electrical properties of P3HT thin films. *Luminescence* **2021**, *36*, 761–768. [[CrossRef](#)]
87. Almohammed, A.; Khan, M.T.; Benghanem, M.; Aboud, S.W.; Shkir, M.; AlFaify, S. Elucidating the impact of PbI₂ on photophysical and electrical properties of poly(3-hexylthiophene). *Mater. Sci. Semicond. Process.* **2020**, *120*, 105272. [[CrossRef](#)]
88. Khan, M.T.; Shkir, M.; Yahia, I.S.; Almohammed, A.; AlFaify, S. An impact of Cr-doping on physical properties of PbI₂ thin films facilely deposited by spin coating technique. *Superlattices Microstruct.* **2020**, *138*, 106370. [[CrossRef](#)]
89. Khan, M.T.; Shkir, M.; Alhour, B.; Almohammed, A.; Ismail, Y.A. Modulation of optical, photophysical and electrical properties of poly(3-hexylthiophene) via Gd:CdS nanoparticles. *Optik* **2022**, *260*, 169092. [[CrossRef](#)]

Disclaimer/Publisher's Note: The statements, opinions and data contained in all publications are solely those of the individual author(s) and contributor(s) and not of MDPI and/or the editor(s). MDPI and/or the editor(s) disclaim responsibility for any injury to people or property resulting from any ideas, methods, instructions or products referred to in the content.